

Inhibition of Tgf β signaling by endogenous retinoic acid is essential for primary lung bud induction

Felicia Chen¹, Tushar J. Desai², Jun Qian¹, Karen Niederreither³, Jining Lü¹ and Wellington V. Cardoso^{1,*}

Disruption of retinoic acid (RA) signaling during early development results in severe respiratory tract abnormalities, including lung agenesis. Previous studies suggest that this might result from failure to selectively induce fibroblast growth factor 10 (*Fgf10*) in the prospective lung region of the foregut. Little is known about the RA-dependent pathways present in the foregut that may be crucial for lung formation. By performing global gene expression analysis of RA-deficient foreguts from a genetic [retinaldehyde dehydrogenase 2 (*Raldh2*)-null] and a pharmacological (BMS493-treated) mouse model, we found upregulation of a large number of Tgf β targets. Increased Smad2 phosphorylation further suggested that Tgf β signaling was hyperactive in these foreguts when lung agenesis was observed. RA rescue of the lung phenotype was associated with low levels of Smad2 phosphorylation and downregulation of Tgf β targets in *Raldh2*-null foreguts. Interestingly, the lung defect that resulted from RA-deficiency could be reproduced in RA-sufficient foreguts by hyperactivating Tgf β signaling with exogenous TGF β 1. Preventing activation of endogenous Tgf β signaling with a pan-specific TGF β -blocking antibody allowed bud formation and gene expression in the lung field of both *Raldh2*-null and BMS493-treated foreguts. Our data support a novel mechanism of RA-Tgf β -Fgf10 interactions in the developing foregut, in which endogenous RA controls Tgf β activity in the prospective lung field to allow local expression of *Fgf10* and induction of lung buds.

KEY WORDS: Retinoic acid, Fgf10, Fibroblast growth factor, Tgf β , Transforming growth factor, Lung development, Foregut development, Organogenesis, Mouse, *Raldh2* (*Aldh1a2*)

INTRODUCTION

During foregut development, activation of morphogenetic programs in the pre-patterned endoderm gives rise to a number of gut-derived organs, including the lung. In the developing mouse, the thyroid and liver primordia arise at around embryonic day (E) 8.5, whereas the lung and pancreatic primordia appear at E9.5 (Wells and Melton, 1999).

Respiratory progenitors (lung and trachea) can be identified in the foregut by E9.0 as a group of endodermal cells posterior to the thyroid that expresses the transcription factor Nkx2.1 (also known as *Titf1* – Mouse Genome Informatics) (Minoo et al., 1999). Subsequently, Fgf10, a fibroblast growth factor that is crucial for budding, is expressed locally in the mesoderm adjacent to these Nkx2.1-expressing endodermal cells to trigger Fgf receptor 2b (Fgfr2b) signaling, resulting in primary lung bud formation. Once primary lung buds form, epithelial tubules undergo extensive branching morphogenesis, which ultimately results in the formation of the bronchial tree and the future alveolar region of the lung (Cardoso and Lu, 2006; Shannon and Hyatt, 2004).

Lung morphogenesis depends on complex interactions between local signals present in this prespecified foregut endoderm and signals from the adjacent mesoderm (Cardoso and Lu, 2006; Shannon and Hyatt, 2004). The mechanisms that control gene expression and cellular activities in the lung field of the foregut at the onset of lung development are still poorly understood. Several studies have implicated retinoic acid (RA) signaling as a key

regulator of these functions during development of the foregut and its derivatives. Genetic deletion of retinaldehyde dehydrogenase 2 (*Raldh2*; also known as *Aldh1a2* – Mouse Genome Informatics), an enzyme essential for RA synthesis in the mouse embryo, results in multiple organ defects and death at around E10.5 (Niederreither et al., 1999). RA signals through nuclear receptors Rars and Rxrs (each with isotypes α , β and γ), which are found as heterodimers bound to RA-responsive elements (RAREs) of target genes (Chambon, 1996). These receptors are expressed in the developing lung from its earliest stages (Mollard et al., 2000b); double-null mutant (*Rara/Rarb* or *Rara/Rarb*) mice show several features previously described in vitamin A-deficient animals (Chambon, 1996; Clagett-Dame and DeLuca, 2002; Kastner et al., 1997; Mendelsohn et al., 1994; Wilson et al., 1953). Maternal deficiency of vitamin A results in dramatic abnormalities in the respiratory system of the embryo, which include tracheoesophageal fistula, lung hypoplasia and lung agenesis (Dickman et al., 1997).

In the developing lung, RA synthesis and utilization are most prominent when primary buds are emerging from the primitive foregut (Malpel et al., 2000). Treatment of the whole E8.5 mouse embryo or isolated E8.5 foregut explants with the pan-RA receptor (RAR) antagonist BMS493 completely abrogates development of the lung and the neighboring stomach (Desai et al., 2004; Mollard et al., 2000a). We found that this phenotype results from failure to induce *Fgf10* expression in the foregut mesoderm at the prospective lung field. The regulation of *Fgf10* by RA occurs within a defined developmental window and is not seen in other foregut derivatives (such as thyroid and pancreas), where Fgf10 is also required for normal development (Desai et al., 2004). These observations have been confirmed in *Raldh2*^{-/-} mice and vitamin A-deficient rats (Desai et al., 2004; Desai et al., 2006; Wang et al., 2006). Furthermore, we have shown that RA is not required for the initiation of lung endodermal cell fate in the foregut (Desai et al., 2006).

¹Pulmonary Center, Boston University School of Medicine, Boston, MA 02118, USA.

²Biochemistry Department, Stanford University, Stanford, CA 94305, USA. ³Baylor College of Medicine, Houston, TX 77030, USA.

*Author for correspondence (e-mail: wcardoso@bu.edu)

These studies raised the intriguing possibility that at the onset of lung development, RA-responsive genes are selectively activated or repressed in the prospective lung field of the foregut to allow bud formation. It was not known which genes present in the developing foregut could be involved in this process. Here we addressed this problem using oligonucleotide microarray and functional analyses in the models of RA deficiency that we had previously characterized, and at a stage in which lung development is crucially dependent on the RA status of the embryo. We provide evidence of a novel regulatory mechanism implicating RA, transforming growth factor β (Tgfb) and Fgf10 interactions in primary lung bud induction. Our results suggest that at the onset of lung development, endogenous RA controls Tgfb signaling in the prospective lung field of the foregut to allow *Fgf10* expression and induction of primary lung buds.

MATERIALS AND METHODS

Raldh2-null, *RARElacZ* reporter, and *Fgf10lacZ* reporter mice

Raldh2-null mutants were characterized previously (Niederreither et al., 1999). *Raldh2*^{-/-} homozygous embryos were distinguished from their heterozygous and wild-type (WT) littermates by their distinct phenotypic features and by genotyping by PCR (Niederreither et al., 1999). Detection of RA signaling was achieved using the *RARElacZ* reporter mouse line. These mice carry the bacterial *lacZ* gene under the control of a heat shock protein promoter (*Hsp68*) and RAREs from the *Rarb* promoter (Rossant et al., 1991). X-Gal staining is used to visualize *lacZ* expression (Malpel et al., 2000). *Fgf10lacZ* reporter mice have been reported previously (Kelly et al., 2001). In this mutant, a myosin light chain-*lacZ* (*Mlc1v-nlacZ-24*) transgene was integrated upstream of *Fgf10*, which allows control of *lacZ* expression by *Fgf10* regulatory sequences; X-Gal staining reveals sites of *Fgf10* expression in the embryo, including the lung (Mailleux et al., 2005). For all experiments, conclusions were based on the evaluation of three independent specimens per culture condition.

Foregut explant cultures

The foregut culture system has been reported previously (Desai et al., 2004; Desai et al., 2006). Briefly, timed-pregnant mice were sacrificed at E8.5 and foreguts were isolated from the embryos (8- to 12-somite stage) in phosphate-buffered saline (PBS) using tungsten needles. Extra-embryonic tissues and dorsal structures were removed. Explants were cultured for 1-3 days on 6-well Transwell-Col dishes (Costar) containing 1.5 ml of BGJb medium (Gibco-BRL), 0.3 mg of vitamin C (Sigma) and 10% fetal calf serum (FCS, Gibco-BRL) with or without the specific modulators of RA or Tgfb signaling (see below). Cultures were shielded from light and incubated at 37°C in 95% air and 5% CO₂. Media were changed daily. Under control conditions, lung buds, stomach and pancreas formed within 24 hours of culture. In some experiments, heparin beads soaked in 100 ng/ml FGF10 (R&D systems) or PBS buffer were grafted onto the foregut after 24 hours of culture.

Modulation of RA and Tgfb signaling

BMS493 (Bristol Meyers Squibb), a pan-RAR antagonist, dissolved in BGJb medium (10⁻⁶ M) was used to antagonize RAR-dependent signaling, as previously reported in this and other systems (Mollard et al., 2000b; Wendling et al., 2000). All-trans RA (Sigma) dissolved in BGJb medium (10⁻⁷ M) was used to rescue RA signaling in *Raldh2*^{-/-} foreguts in culture. Foreguts were treated for 3 days with recombinant human TGF β 1 (5-20 ng/ml, R&D Systems) or a pan-specific TGF β -blocking antibody (200 μ g/ml, R&D Systems) dissolved in BGJb medium to activate or inhibit Tgfb signaling, respectively.

Microarray analysis of RA-responsive genes in the developing foregut

E8.5 WT (control and BMS493-treated, *n*=3 each) and *Raldh2*^{-/-} (control and RA-treated, *n*=3 each) foreguts were cultured for 24 hours. Total RNA was isolated using the RNeasy Kit (Qiagen), and subjected to amplification, labeling, and fragmentation according to Affymetrix's recommendations. cRNA was hybridized to Affymetrix's Mouse Genome 430 2.0 array chips. Three array chips were used per experimental condition. A single weighted

mean expression level for each gene per condition along with a detection *P* value was calculated using Affymetrix Microarray Suite 5.0 software. Data from each array were scaled to the target intensity of 500 to normalize the results for inter-array comparisons. Quality control parameters of each chip met the acceptable criteria provided by Affymetrix. Genes with detection *P* values greater than 0.05 (considered to be 'absent') in all twelve chips were eliminated from the analysis. Gene expression profiles were compared (WT control versus BMS493; *Raldh2*^{-/-} control versus RA). The difference in expression of each gene was considered to be significant if the *P* value was lower than 0.05 (Cyber *t*-test, <http://visitor.ics.uci.edu/genex/cybert>). To further increase the specificity of the analysis, only genes whose expression levels were significantly changed in both comparisons were retained on the final list of potential RA targets.

Western blotting

After 24 hours of culture, the heart of the foregut explant was separated from the foregut region and discarded. The protein extract from individual foregut explants was subjected to SDS-PAGE, blotted onto nitrocellulose, washed in TBST [Tris-buffered saline (TBS) with 0.1% Tween 20], blocked with 5% milk in TBST, and incubated with polyclonal antibody (1:400) to phosphorylated Smad2 (pSmad2, Cell Signaling) in TBST with 5% milk overnight. The Immun-Star HRP Chemiluminescent Kit (Bio-Rad) was used for signal development according to the manufacturer's instructions. Total Smad2 (tSmad2, Cell Signaling) was used for normalization.

Whole-mount in situ hybridization

Whole-mount in situ hybridization (WMISH) of explants and embryos was performed in a 96-well plate as previously described (Lu et al., 2004; Wertz and Herrmann, 2000). Briefly, digoxigenin (DIG)-labeled riboprobes (Maxiscript kit, Ambion) were generated and amplified from total embryonic cDNA (*Colla2*, *Ctgf*, *Tgfb2*, *Tgfb1*, *Tgfb3*) or plasmids carrying cDNA for the genes of interest (*Tgfb1*, *Nkx2.1*, *Sftpc*, *Fgf10*, *Tgfb3*, *Tgfb1*). Specimens were rehydrated, digested with proteinase K (Boehringer Mannheim), prehybridized (1 hour, 70°C) in buffer containing 50% formamide, 5 \times SSC, 1% SDS, 50 mg/ml yeast RNA and heparin followed by overnight hybridization with DIG-labeled RNA probes, and another overnight incubation with anti-DIG alkaline phosphatase conjugate (Boehringer Mannheim) at 4°C. Signal was visualized with BM Purple substrate (Roche Diagnostics). Conclusions were based on the evaluation of at least three independent specimens per probe per condition.

Immunohistochemistry

Tissues were fixed in 4% paraformaldehyde in PBS overnight at 4°C, washed twice in TBS with 0.1% Triton X-100 (Sigma), and blocked for 1 hour in blocking buffer (1 \times TBS with 5% donkey sera, 0.1% Triton X-100). Samples were incubated with primary antibody in blocking buffer overnight [1:150 dilution of rabbit anti-mouse pSmad2 antibody (Cell Signaling), 1 μ g/ml sheep anti-mouse Tgfb1 antibody (R&D systems)] at 4°C, washed for 1 hour and incubated with secondary antibody overnight (1:750 donkey anti-rabbit antibody conjugated to AF488 and donkey anti-sheep antibody conjugated to AF598, both from Molecular Probes), washed five times for 1 hour each in blocking buffer, then stored in SlowFade Gold Antifade buffer (Molecular Probes) and photographed with a laser confocal microscope.

Mesenchymal lung cell culture and real-time PCR

Mouse neonatal lung mesenchymal (MLg) cells were cultured in DMEM, 10% FCS with or without the specified modulator (all-trans RA or TGF β 1) for 8-24 hours (*n*=3 100-mm dish plates per condition). Total RNA was isolated (Trizol, Invitrogen), reverse transcribed (1 μ g RNA) and amplified by real-time PCR (SYBR Green qPCR Kit, Applied Biosystems). A dissociation curve was used to determine the relative concentration of the single PCR product. 18S RNA was used for normalization.

Cell proliferation and cell death assay

Cell proliferation was assessed by expression of PCNA protein (PCNA Staining Kit, Zymed). Apoptosis was evaluated by TUNEL (ApopTag Plus, Chemicon). These assays were performed in paraffin sections (5 μ m) of foregut explants according to the manufacturers' recommendations. Sections were counterstained with Methyl Green.

RESULTS

The Tgfb pathway is regulated by endogenous RA at the onset of lung development

To identify RA-dependent pathways potentially involved in lung bud initiation, we generated global transcriptional profiles of foregut explants in which lung formation occurred (RA-sufficient) or was abrogated by disruption of RA signaling (RA-deficient). For this we used both the pharmacologic (BMS493) and the genetic (*Raldh2*^{-/-}) models of RA deficiency that we had previously characterized. In the pharmacologic model, RA signaling was antagonized in E8.5 (8- to 12-somite stage) foreguts by treatment with BMS493; this prevented lung bud formation (Desai et al., 2004). In the genetic model, *Raldh2*^{-/-} foreguts were similarly cultured in control medium (in which no lung forms) or in medium containing RA (10⁻⁷ M), which allowed lung formation in these mutants (Desai et al., 2006).

Microarray analysis was performed on RNA isolated from these samples (as described in Materials and methods). Modulation of RA signaling was confirmed by altered expression of known RA targets, such as *Rarb*, *Hoxa1* and *Hoxb1* (Chambon, 1996; Niederreither et al., 1999). A comprehensive description of these transcriptional profiles will be reported elsewhere. Analysis of these profiles using the EASE (Expression Analysis Systematic Explorer, <http://david.abcc.ncifcrf.gov>) software revealed a striking overrepresentation of 'Tgfb signaling pathway-related genes' upregulated in the RA-deficient foreguts ($P=0.009$). This list was expanded, as we searched for additional Tgfb targets based on published reports (Table 1, description below).

To determine whether the upregulation of Tgfb targets in the RA-deficient foreguts reflected an overall hyperactivation of Smad-mediated signaling by Tgfb1-3, we assessed levels of phosphorylated and total Smad2 in all groups by western blotting. As anticipated, Smad2 phosphorylation was consistently higher in RA-deficient foreguts compared with their respective RA-sufficient controls (Fig. 1A). Thus, we concluded that disruption of RA signaling leads to an abnormal hyperactivity of the Tgfb pathway in the developing foregut.

Tgfb targets identify sites of Tgfb hyperactivation in the mesoderm of RA-deficient foreguts

The Tgfb targets upregulated in RA-deficient foreguts encode a diverse group of molecules, and include several mediators of the fibrogenic activities of Tgfb [connective tissue growth factor (*Ctgf*),

cysteine rich protein 61 (*Cyr61*), procollagen type I alpha 2 (*Col1a2*), procollagen type III alpha 1 (*Col3a1*), procollagen C-endopeptidase enhancer protein (*Pcolce*), tissue inhibitor of metalloproteinase 1 and 3 (*Timp1* and *Timp3*, respectively)], secreted proteins [biglycan (*Bgn*), transforming growth factor β induced (*Tgfb1*), secreted acidic cysteine rich glycoprotein (*Sparc*), secreted phosphoprotein 1 (*Spp1*)], cell surface receptors [CD44 antigen (*Cd44*)], transcription factors [activating transcription factor 3 (*Atf3*)], colony stimulating factor (*Csf1*), as well as insulin-like growth factor binding protein 4 (*Igfbp4*) (see Table 1 for references).

Previous studies and an initial assessment of the expression pattern of these genes at the onset of lung development showed them to be predominantly transcribed in mesodermal tissues (Chuva de Sousa Lopes et al., 2004; Ferguson et al., 2003; Ponticos et al., 2004). The presence of these targets in the mesoderm, where *Raldh2* and *RARElacZ* are also expressed (Malpel et al., 2000), suggests that RA and Tgfb pathways interact locally in the foregut. Thus, we assessed expression of three representative Tgfb targets, *Tgfb1*, *Ctgf* and *Col1a2*, in our system.

Tgfb1 (also called β ig-h3) is a 68 kDa secreted cell-adhesion molecule, known to bind collagen, fibronectin and sulfated glycosaminoglycans, which has been shown to be induced by TGF β 1 in various cells lines (Billings et al., 2002; Skonier et al., 1994). First, we validated *Tgfb1* as a read out of Tgfb activation in lung mesoderm-derived cells (MLg) by showing a dose-dependent induction of *Tgfb1* at 8 hours with recombinant TGF β 1 treatment (Fig. 1B). Then, to investigate the RA-*Tgfb1* relationship in the foregut, we compared sites of Rar-dependent signaling and *Tgfb1* transcription by X-Gal staining of *RARElacZ* reporter mice and WMISH of *Tgfb1*, respectively. In wild-type (WT) control cultures, *Tgfb1* was localized to the foregut mesoderm associated with the proximal (stalk) region of lung primordium, where RA signaling was reported by *lacZ* expression (Fig. 1C-E).

BMS493 disruption of RA signaling abolished *RARElacZ* expression and resulted in strong *Tgfb1* signals in the foregut mesoderm, particularly obvious where the lung bud and stomach failed to form ($n=6$) (Fig. 1G-I). Immunostaining of *Tgfb1* showed a marked increase of *Tgfb1* protein locally in the lung field; the broader domain of expression, compared with that of mRNA, suggested accumulation that is likely to be due to a longer half-life of *Tgfb1* protein. The stronger pSmad2 staining in BMS493-treated foreguts

Table 1. Tgfb targets upregulated in retinoic acid-deficient foreguts

Gene	WT (BMS493/Ctrl)		<i>Raldh2</i> ^{-/-} (Ctrl/RA)		References
	FC*	P	FC#	P	
<i>Atf3</i>	1.5	2×10 ⁻³	1.6	8×10 ⁻⁵	(Kang et al., 2003; Yun et al., 2002)
<i>Bgn</i>	2.5	1×10 ⁻⁴	2.5	2×10 ⁻⁵	(Benson et al., 2002; Chen et al., 2002; Groth et al., 2005; Ungefroren et al., 2003)
<i>Cd44</i>	1.8	5×10 ⁻⁵	1.5	7×10 ⁻³	(Verrecchia et al., 2001)
<i>Cdc42</i>	1.7	2×10 ⁻⁵	1.3	1×10 ⁻²	(Verrecchia et al., 2001)
<i>Col1a2</i>	2.1	2×10 ⁻⁵	2.0	5×10 ⁻⁵	(Benson et al., 2002; Kapoun et al., 2004; Okano et al., 2006; Verrecchia et al., 2001)
<i>Col3a1</i>	1.2	2×10 ⁻²	3.5	8×10 ⁻³	(Benson et al., 2002; Bertelli et al., 1998; Verrecchia et al., 2001)
<i>Csf1</i>	1.7	3×10 ⁻³	1.5	1×10 ⁻²	(Xie et al., 2003)
<i>Ctgf</i>	3.6	1×10 ⁻⁹	1.3	3×10 ⁻²	(Benson et al., 2002; Colwell et al., 2006; de Jong et al., 2002; Kapoun et al., 2004)
<i>Cyr61</i>	1.4	1×10 ⁻³	1.7	8×10 ⁻⁷	(Bartholin et al., 2007; Benson et al., 2002; de Jong et al., 2002; Leivonen et al., 2005)
<i>Igfbp4</i>	1.6	3×10 ⁻³	1.3	8×10 ⁻⁴	(Benson et al., 2002; Dahlfors and Arnqvist, 2000; Verrecchia et al., 2001)
<i>Pcolce</i>	1.6	2×10 ⁻⁵	1.4	4×10 ⁻⁴	(Shalitin et al., 2003)
<i>Sparc</i>	1.5	1×10 ⁻⁴	1.2	9×10 ⁻³	(Benson et al., 2002; Fujita et al., 2002; Pavasant et al., 2003)
<i>Spp1</i>	8.8	2×10 ⁻⁴	3.3	2×10 ⁻²	(Benson et al., 2002; Sodek et al., 1995)
<i>Tgfb1</i>	4.1	2×10 ⁻¹⁰	8.7	6×10 ⁻¹⁴	(Benson et al., 2002; LeBaron et al., 1995; Schneider et al., 2002; Skonier et al., 1994)
<i>Timp1</i>	1.4	6×10 ⁻³	1.9	5×10 ⁻⁵	(Verrecchia et al., 2001)
<i>Timp3</i>	1.3	3×10 ⁻²	1.5	8×10 ⁻³	(de Jong et al., 2002; Kapoun et al., 2004; Verrecchia et al., 2001)

FC*, fold change ratio between the expression levels in BMS493-treated and untreated WT foreguts.

FC#, fold change ratio between the expression levels in untreated and RA-treated *Raldh2*^{-/-} foreguts.

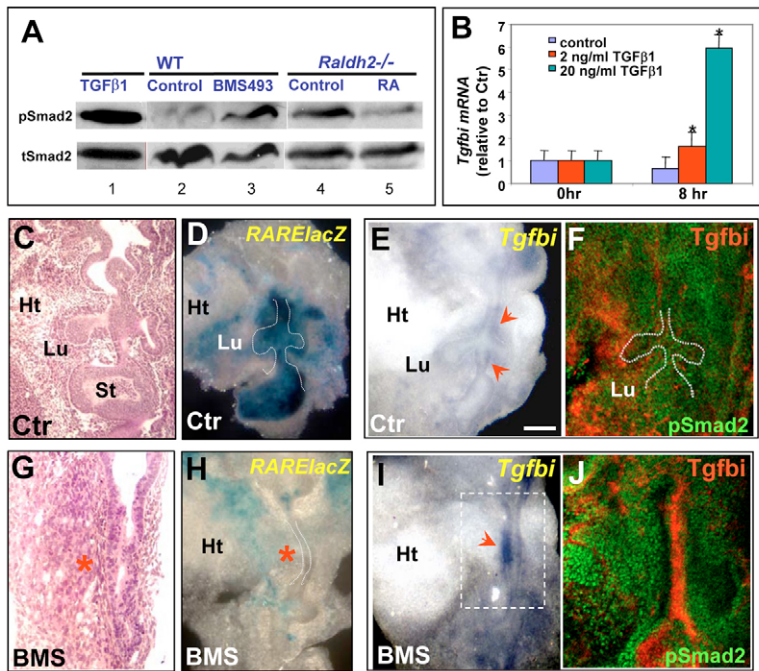


Fig. 1. The *Tgfβ* pathway is regulated by RA at the onset of lung development. (A) Western blotting of cultured mouse foregut explants (E8.5 plus 24 hours) revealing increased phosphorylation of Smad2 (pSmad2) in RA-deficient conditions (lane 3, BMS493-treated WT; lane 4, non-RA-supplemented *Raldh2*^{-/-}) as compared with RA-sufficient conditions (lane 2, WT control; lane 5, RA-supplemented *Raldh2*^{-/-}). TGFβ1-treated WT foregut is used as a positive control (lane 1). Total Smad2 (tSmad2) is used for normalization. (B) Real-time PCR showing rapid dose-dependent induction of *Tgfbi* in TGFβ1-treated lung mesenchymal cells (MLg cells; asterisks indicate $P < 0.05$ by Student's *t*-test). (C, G) Hematoxylin and Eosin (H&E) staining of paraffin-embedded sections showing lung bud formation in the control, but not in the BMS493-treated foregut culture. (D, H) *RARElacZ* expression is strong in control foregut cultures, but is dramatically suppressed by BMS493 treatment (asterisk marks the presumptive lung region in G, H). (E, F, I, J) Whole-mount in situ hybridization (WMISH) and immunostaining of control foreguts revealing a low level of *Tgfbi* mRNA (E, arrowheads) and *Tgfbi* protein (F, red) expression in the foregut mesoderm of the lung primordium. BMS493 treatment results in increased *Tgfbi* mRNA (I, arrowhead) and protein (J, red) in the mesoderm of the presumptive lung and stomach fields, and stronger pSmad2 signals, as compared with the control (F, J, green). Ht, heart; Lu, lung; St, stomach; Ctr, control. Scale bar: 300 μm in E.

compared with controls, as revealed by confocal image analysis, further suggested an association between increased *Tgfbi* expression and hyperactivation of Tgfβ signaling (Fig. 1F, J). The negative spatial correlation between *Tgfbi* and RA-dependent signaling was further supported by comparing the expression of *Tgfbi* and *RARElacZ* in E9.0-9.5 embryos. In WT embryos, *Tgfbi* transcripts were almost undetectable in the *RARElacZ*-expressing region that encompasses most of the foregut (Fig. 2A, B; see also Fig. 2C, asterisk on the right). This contrasted with the abundant *Tgfbi* signals

observed in the corresponding region of *Raldh2*^{-/-} mice in vivo (Fig. 2C, arrowhead on the left), or in *Raldh2*^{-/-} foreguts cultured without RA supplementation (Fig. 2D). Although in *Raldh2*^{-/-} explants *Tgfbi* signals were highly induced in both thyroid and lung fields, bud formation and *Nkx2.1* expression were disrupted only in the lung field (Fig. 2D, E). Strikingly, *Tgfbi* signals were dramatically reduced in *Raldh2*^{-/-} foregut explants in which exogenous RA rescued budding and expression of *Nkx2.1* in the lung field (Fig. 2F, G). Independent evidence that activation of RA signaling (by treatment with RA

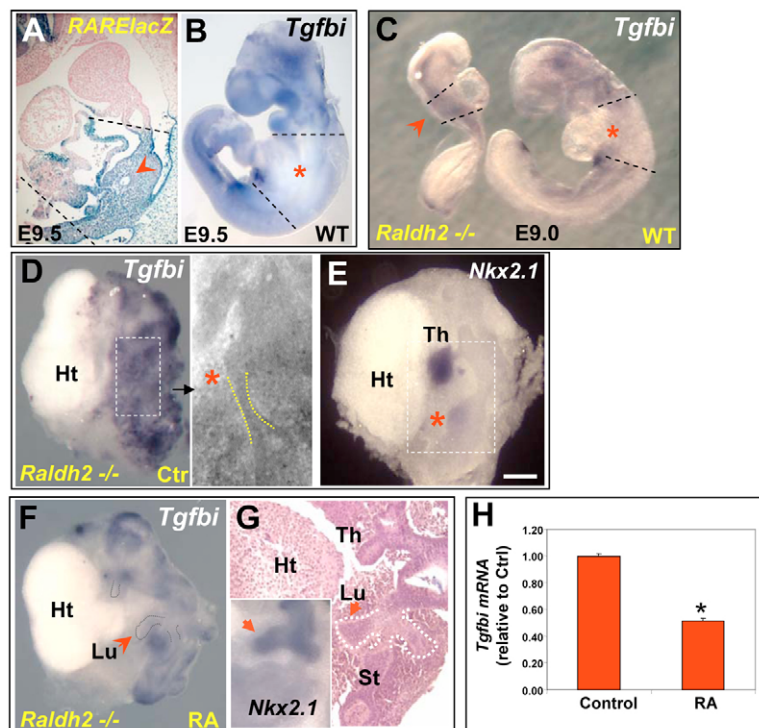


Fig. 2. Expression of *Tgfbi*, a target of the Tgfβ pathway, under RA-sufficient and -deficient conditions. (A-C) X-Gal staining of E9.5 *RARElacZ* mouse embryo showing strong signals in the foregut region (A, between the dashed lines), where *Tgfbi* expression is minimal by WMISH (asterisk in B, C, between dashed lines). By contrast, *Tgfbi* signals are significantly stronger in the same region of the *Raldh2*^{-/-} foregut in vivo (C, arrowhead), compared with a WT littermate. (D) WMISH showing high levels of expression of *Tgfbi* in a non-RA-supplemented *Raldh2*^{-/-} foregut explant. The *Tgfbi* expression domain depicted in the boxed area includes the thyroid (Th) and the region where the lung failed to form. (E) WMISH of *Nkx2.1* in *Raldh2*^{-/-} control cultures. Asterisk (in the enhanced-contrast image of the explant, D, right; E) marks the presumptive lung field. (F, G) *Tgfbi* expression is dramatically reduced in *Raldh2*^{-/-} foregut in which lung (Lu) bud formation was rescued by RA supplementation (F, arrowhead). H&E staining of paraffin-embedded section of RA-supplemented *Raldh2*^{-/-} reveals bud formation in the presumptive lung region of the foregut (G, arrowhead). The presence of lung bud formation is further confirmed by WMISH of *Nkx2.1* in RA-supplemented *Raldh2*^{-/-} foregut (G, inset, arrowhead). Dotted lines outline the lung. (H) Real-time PCR showing downregulation of *Tgfbi* in RA-treated lung mesenchymal (MLg) cells (*, $P < 0.05$ by Student's *t*-test). Ht, heart; St, stomach; Ctr, control. Scale bar: 300 μm in E.

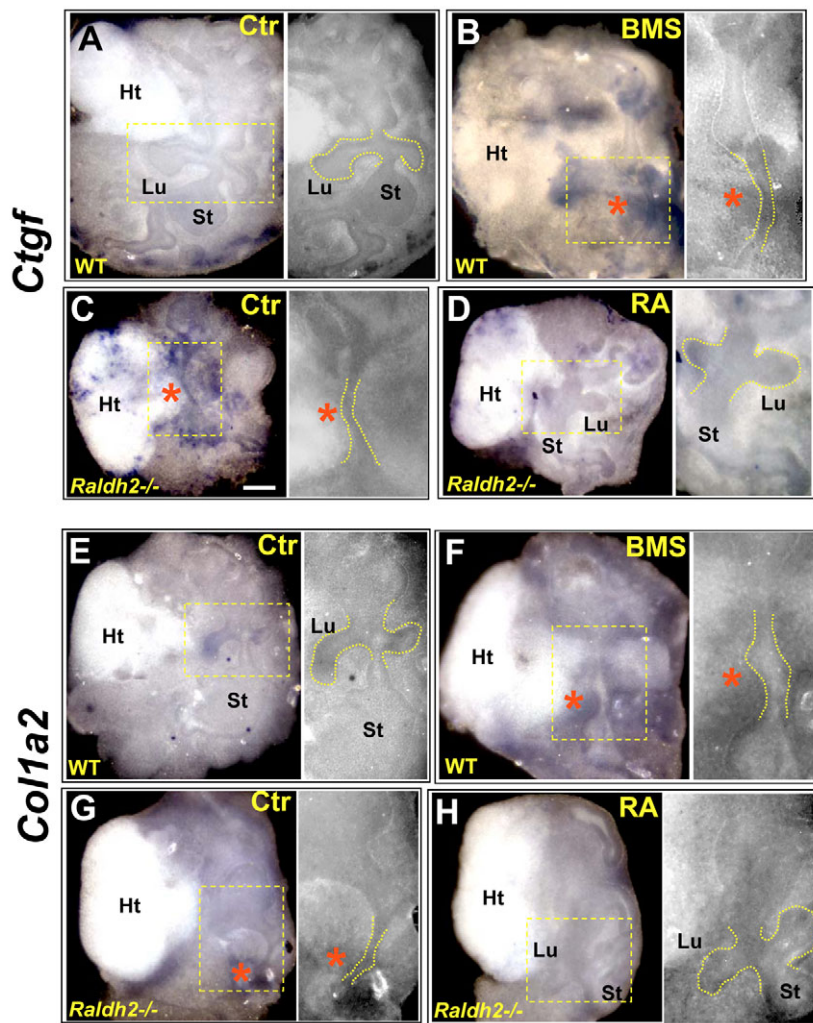


Fig. 3. *Ctgf* and *Col1a2* are Tgfb targets upregulated in RA-deficient mouse foreguts.

Each panel depicts WMISH (left) and the corresponding black and white enhanced-contrast image of the explants (right). Boxes outline the region that includes the lung domain. (A–D) WMISH reveals no *Ctgf* signals in the WT control foregut (A), but expression is significantly upregulated in the mesoderm at the presumptive lung region of the BMS493-treated foregut (B, asterisks) and non-RA-supplemented *Raldh2*^{-/-} foregut (C, asterisks). *Ctgf* expression is markedly suppressed by RA supplementation in *Raldh2*^{-/-} foregut (D). (E–H) *Col1a2* expression is detected by WMISH in the mesoderm of WT control lung bud (E) and is also dramatically increased in BMS493-treated foreguts (F, asterisks) and in non-RA-supplemented *Raldh2*^{-/-} foreguts (G, asterisks). Expression of *Col1a2* is markedly downregulated by addition of exogenous RA in *Raldh2*^{-/-} foregut (H). Ht, heart; Lu, lung; St, stomach; Ctr, control. Scale bar: 300 μm in C.

10^{-7} M) inhibits *Tgfb1* expression in lung mesoderm-derived MLg cells (which also respond to TGFβ1) is provided in Fig. 2H. *Tgfb1* levels are not affected by BMS493 treatment in these cells, as they lack endogenous RA signaling (data not shown).

WMISH analysis of other Tgfb targets, such as *Ctgf* and *Col1a2*, in these explants revealed a similar influence of RA status on their expression pattern. *Ctgf* is a CCN-family member (along with *Cyr61*) and an immediate early response gene product induced by Tgfb (Leask and Abraham, 2003). *Col1a2* is one of the subunits of type I collagen, which represents a major structural component of most connective tissues (Olsen et al., 2003). *Ctgf* signals could not be identified in the WT control foreguts (Fig. 3A), but were dramatically induced in the foregut mesoderm associated with the presumptive lung field of BMS493-treated WT and non-RA-supplemented *Raldh2*^{-/-} foreguts (Fig. 3B,C). Rescue of the lung bud in RA-treated *Raldh2*^{-/-} cultures was associated with a marked decline in *Ctgf* expression (Fig. 3D). Analysis of *Col1a2* expression showed a similar behavior under the experimental conditions described above (Fig. 3E–H).

TGFβ1-treated foreguts fail to develop lung

We reasoned that if hyperactivation of Tgfb signaling in the foregut was responsible for the disruption of lung formation in RA-deficient explants, a similar effect should be observed by directly applying Tgfb protein to RA-sufficient foreguts. TGFβ1 was

chosen because of its ability to stimulate Smad2 phosphorylation (Fig. 1A, lane 1) and because of its overall abundance in mesoderm-derived tissues (Schmid et al., 1991). Foregut treatment with 5 ng/ml of recombinant TGFβ1 resulted in only a small endodermal pouch where lungs were expected to develop ($n=3$, data not shown). At 20 ng/ml, TGFβ1 consistently blocked induction of lung buds and stomach ($n=15$), reminiscent of the effect seen in BMS493-treated cultures (Fig. 4A,B) (Desai et al., 2004). Tgfb activation was confirmed by widespread induction of *Tgfb1* mRNA and protein throughout the explant (Fig. 4C,D). Unlike BMS493, TGFβ1 affected other foregut-derived structures. For example, albumin gene expression, not altered by BMS493 treatment, was inhibited by TGFβ1 (Desai et al., 2004) (data not shown). The disruption of lung development was confirmed by the absence of the endodermal markers *Nkx2.1* and surfactant associated protein C (*Sftpc*) transcripts in the presumptive lung field of TGFβ1-treated foreguts (Fig. 4I–L). The presence of abundant proliferating cell nuclear antigen (PCNA) and control-like pattern of TUNEL staining in all layers suggested that TGFβ1 was not inducing toxic effects in these explants (Fig. 4E–H and data not shown).

We asked whether the effects above could be secondary to TGFβ1-mediated disruption of RA signaling. This was ruled out by experiments in which *RARElacZ* foreguts were shown to maintain strong *lacZ* signals after 3 hours and 72 hours of culture in TGFβ1-containing medium (Fig. 5A,B).

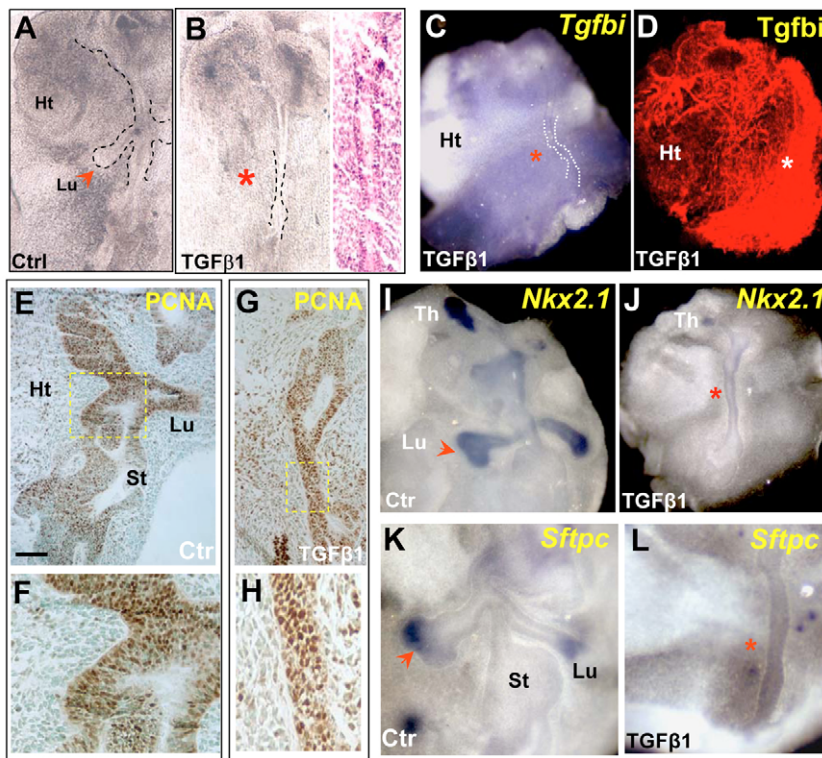


Fig. 4. Hyperactivation of Tgfβ signaling disrupts lung formation in the developing foregut.

(A,B) Treatment of mouse foregut explants with recombinant TGFβ1 results in lung agenesis (B, asterisk). (C,D) WMISH and immunostaining showing generalized induction of *Tgfβi* message (C) and protein (D), in TGFβ1-treated foreguts. (E-H) PCNA staining showing abundant endodermal and mesodermal labeling in both control and TGFβ1-treated foreguts (boxed regions in E,G are magnified in F,H). (I-L) WMISH showing *Nkx2.1* and *Sftpc* in lung buds of controls (I,K, arrowheads), but not in the presumptive lung region of TGFβ1-treated foreguts (J,L, asterisks). Ht, heart; Lu, lung; St, stomach; Th, thyroid; Ctr, control. Scale bar: 200 μm in E.

TGFβ1 disrupts *Fgf10* expression in the foregut mesoderm

Based on the reported role of *Fgf10* in organogenesis (Min et al., 1998; Sekine et al., 1999), we proposed that the disruption of lung bud formation by TGFβ1 was due to loss of *Fgf10* expression in the mesoderm. WMISH analysis confirmed that this was the case, as *Fgf10* expression was almost abolished throughout the TGFβ1-treated foreguts (Fig. 5C,D). The effect did not seem to result from loss of *Fgf10*-expressing mesodermal cells, but rather from downregulation of *Fgf10* expression in these cells. Indeed, treating MLg cells with TGFβ1 also resulted in marked downregulation of *Fgf10* mRNA (Fig. 5E), in agreement with observations in other systems (Beer et al., 1997; Lebeche et al., 1999; Tomlinson et al., 2004). Interestingly, engrafting a heparin bead soaked in FGF10 protein onto TGFβ1-treated foreguts rescued bud outgrowth and *Nkx2.1* expression in the foregut endoderm, in spite of the

widespread hyperactivation of Tgfβ signaling (Fig. 5F,G). This suggests that the effects of TGFβ1 in the prospective lung endoderm are likely to be secondary to the loss of *Fgf10* in the mesoderm, because when *Fgf10* is replaced exogenously, *Fgfr2b* signaling appears to stimulate lung gene expression and growth even in the context of Tgfβ pathway hyperactivation.

Components of the Tgfβ pathway are present in the foregut and early lung

Although our functional assays indicated that Tgfβ gain-of-function is incompatible with lung formation, the question remained whether endogenous Tgfβ signaling was required for lung development. Analysis of pSmad2 in the developing embryo suggests that Tgfβ signaling is present diffusely in the foregut and at a very low level (de Sousa Lopes et al., 2003), in agreement with our findings (Fig. 1F). Expression of components of the Tgfβ

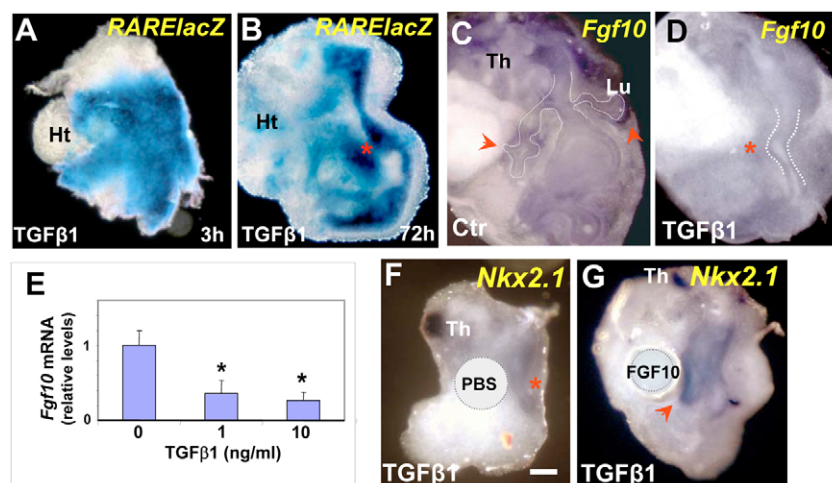


Fig. 5. TGFβ1 disrupts *Fgf10* expression in the mouse foregut mesoderm. (A,B) X-Gal staining of *RARElacZ* foregut cultured in TGFβ1-containing medium reveals strong *RARElacZ* signal at 3 hours (A) and 72 hours (B) in culture. (C,D) *Fgf10* is expressed in control foreguts (C, arrowheads) and is suppressed in TGFβ1-treated foreguts (D, asterisk). (E) Real-time PCR results showing the downregulation of *Fgf10* in MLg cells by TGFβ1 treatment (*, $P < 0.05$ by Student's *t*-test). (F,G) FGF10- but not PBS-soaked heparin bead rescues *Nkx2.1* expression and bud outgrowth in TGFβ1-treated foreguts (G, arrowhead). Ht, heart; Lu, lung; Th, thyroid; Ctr, control. Scale bar: 250 μm in F.

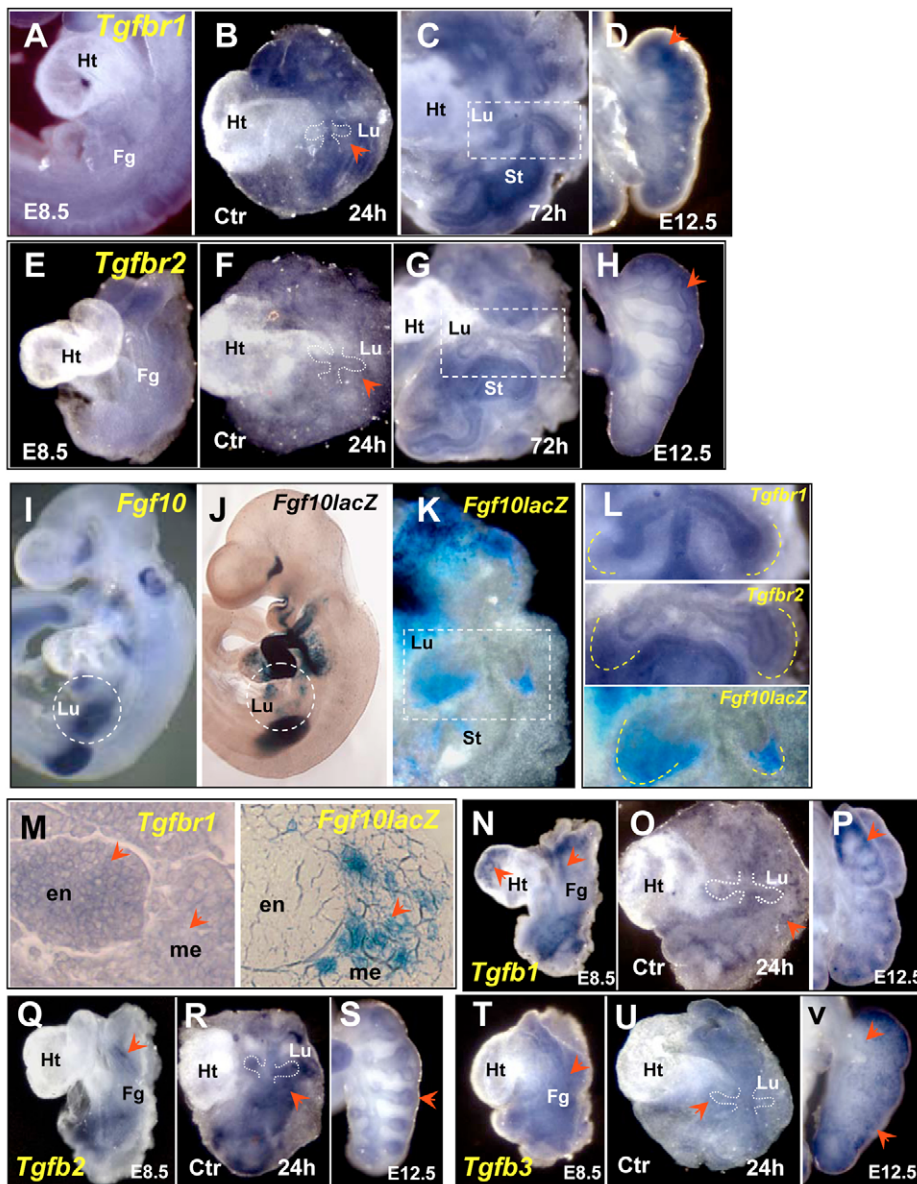


Fig. 6. Expression of Tg β ligands and receptors in the mouse foregut and early lung. (A-H) WMISH of *Tgfb1* and *Tgfb2* showing that both receptors are diffusely expressed in the E8.5 foregut (A,E) and in control cultured foregut at 24 hours (B,F). By 72 hours in culture, strong *Tgfb1* (C) and *Tgfb2* (G) expression is detected in the endoderm and mesoderm of the lung region (boxed areas in C and G, magnified in L). At E12.5, both receptors are highly expressed in the distal lung in vivo (arrows). (I,J) WMISH of *Fgf10* (I) and X-Gal staining of *Fgf10lacZ* (J) expression in E9.5 embryos reveal *Fgf10* expression in the lung region (circled). (K) X-Gal staining of an *Fgf10lacZ* foregut explant at 72 hours showing strong *lacZ* expression in the mesenchyme associated with the distal lung buds. (L) Boxed areas from C, G and K, showing overlap of *Fgf10lacZ*, *Tgfb1* and *Tgfb2* expression in the mesenchyme at the lung field. (M) Histological section of WMISH specimens from L showing localization (arrowheads) of *Tgfb1* and *Fgf10lacZ* expression. (N-V) WMISH of *Tgfb1-3*. Freshly isolated E8.5 explants (N,Q,T) and control 24-hour cultures (O,R,U) show diffuse expression of these ligands in the foregut region, mostly in the mesoderm; signals are in some cases associated with cardiac and vascular structures (*Tgfb1*, arrowheads in N,O; *Tgfb2*, arrowhead in R) or endodermal structures (*Tgfb2* in S), as previously reported. In the E12.5 lung, *Tgfb1* is expressed in the subepithelial mesenchyme (P, arrowhead), *Tgfb2* is mostly restricted to the distal epithelium (S, arrowhead), and *Tgfb3* is present in mesothelial cells of the pleura and distal epithelium and mesenchyme (V, arrowhead). en, endoderm; me, mesoderm; Fg, foregut; Lu, lung; Ht, heart; St, stomach.

pathway has been extensively reported in the developing foregut, although these studies have not focused specifically on the lung domain (Millan et al., 1991; Roelen et al., 1994). To address this issue, we performed a comprehensive expression pattern analysis of the Tg β subfamily ligands (*Tgfb1-3*) and receptors (*Tgfb1-2*) both in vivo (E8.5-9.5 embryo and E12.5 lung) and in foregut cultures. At E8.5, both *Tgfb1* and *Tgfb2* were expressed diffusely in all layers of the foregut (Fig. 6A,E). This diffuse pattern was also seen after 24 hours in culture, but by 72 hours both receptors were predominantly expressed in the foregut endoderm with lower signals in the mesoderm (Fig. 6B,C,F,G,L,M). Strong *Tgfb1/2* signals were detected later in the distal E12.5 lung in vivo (Fig. 6D,H). Interestingly, analysis of *Fgf10* expression either by WMISH or by X-Gal staining of an *Fgf10lacZ* reporter mouse (Kelly et al., 2001; Maillieux et al., 2005) showed that sites where *Fgf10* is induced in the lung field are also enriched in *Tgfb1/2* transcripts (Fig. 6I-M). This suggests that *Fgf10*-expressing mesodermal cells in the lung field are able to respond to Tg β ligands (either endogenous or

exogenous) and activate Tg β signaling. Together with the observations from the previous section, the data further support the idea that Tg β signaling in the mesoderm influences *Fgf10* expression. Which ligands are expressed in the lung field? Fig. 6N-V confirms previous reports showing that the foregut mesoderm expresses *Tgfb1-3* at E8.5 and at 24 hours in culture. Later, *Tgfb2* became more restricted to the epithelium (in the E12.5 lung, Fig. 6S); *Tgfb3* expression could also be seen in the mesoderm and mesothelial surfaces (see pleura in Fig. 6V).

Endogenous Tg β signaling influences local expression of Tg β targets but not lung bud initiation from the foregut

A number of studies have addressed the role of Tg β in vivo and in vitro in lung branching morphogenesis and differentiation. Although the lung does form in mice lacking *Tgfb1*, 2 or 3, uncertainties remain about how functional redundancy or maternal Tg β transfer influence the overall severity of the phenotype (Bartram and Speer, 2004; Cardoso and Lu, 2006; Letterio et al., 1994).

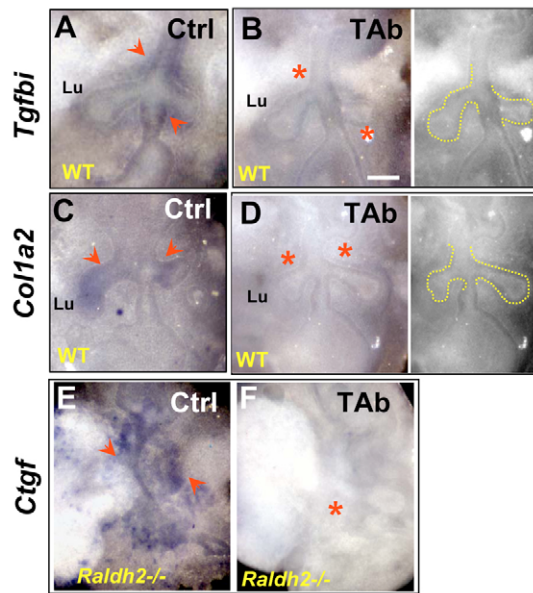


Fig. 7. Effect of TGF β -blocking antibody on *Tgfb1*, *Col1a2* and *Ctgf* expression and lung bud formation. Expression of *Tgfb1* (B) *Col1a2* (D) is noticeably decreased in WT mouse foreguts treated with a pan-specific TGF β -blocking antibody (TAB, asterisks) when compared with foreguts cultured in control medium (A,C, arrowheads). Culturing *Raldh2*^{-/-} foregut in TAB (F, asterisk) prevents the high-level *Ctgf* expression typically seen in the untreated *Raldh2*^{-/-} foregut (E, arrowheads). Lung bud formation in WT foreguts is not affected by the treatment with TAB (B,D). Panels to the right are the corresponding enhanced-contrast images of the explants in B and D. Lu, lung; Ctr, control. Scale bar: 300 μ m in B.

To investigate the role of endogenous Tgf β signaling in lung formation, first we asked whether we could reliably prevent activation of signaling by all Tgf β subfamily ligands in our foregut explants. For this, we cultured E8.5 foreguts in medium containing a pan-specific TGF β -blocking antibody (referred to here as TAB) or control isotype-matched immunoglobulins. Changes in expression of pSmad2 in TAB-treated explants could not be detected, given that pSmad2 signals were already relatively low in untreated WT foreguts. To circumvent this problem, we used WMISH to assess expression of the Tgf β targets *Tgfb1*, *Col1a2* and *Ctgf* as ‘reporters’ of Tgf β activity in these cultures. *Tgfb1* and *Col1a2* transcripts were significantly reduced in WT foregut explants treated with TAB (200 μ g/ml) (Fig. 7A-D). Efficient inhibition of Tgf β signaling was also suggested by the dramatic reduction in the *Ctgf* levels observed in *Raldh2*^{-/-} foreguts cultured in TAB-containing medium (Fig. 7E,F, also compare with WT in Fig. 3A). Analysis of TAB-treated WT foreguts showed that blocking endogenous Tgf β signaling does not interfere with primary lung bud formation. This was in full agreement with results from *Tgfb*-knockout mouse models (Bartram and Speer, 2004), and further supported the idea that an excess, but not deficiency, of Tgf β function is deleterious to early lung bud morphogenesis.

Lung bud formation is partially rescued by blocking Tgf β signaling in RA-deficient foreguts

Our data suggested that the increased activation of the Tgf β pathway could play a major role in the abrogation of lung development of RA-deficient foreguts. If this is the case,

suppressing the overactive Tgf β signaling in the RA-deficient foreguts should lead to lung bud formation in both *Raldh2*^{-/-} and BMS493 models. To test this hypothesis, E8.5 foregut explants were cultured in media containing BMS493 alone, or BMS493 mixed with either isotype-control antibody (CAB) or TAB (200 μ g/ml). *Nkx2.1* expression was used to identify lung progenitor cells in the foregut endoderm and nascent lung buds. As previously reported, BMS493 cultures failed to induce lung buds or express proper levels of *Nkx2.1* ($n=13/13$) (Desai et al., 2004) (Fig. 8A). By contrast, bud formation and high levels of *Nkx2.1* expression were consistently observed in BMS493 plus TAB-treated WT foreguts ($n=13/13$) (Fig. 8B). TAB also seemed to have rescued the formation of the stomach ($n=13/13$), which is suppressed by BMS493 (Desai et al., 2004). Remarkably, suppression of Tgf β signaling by TAB was also effective in rescuing bud formation and *Nkx2.1* expression in the lung field of *Raldh2*^{-/-} foreguts ($n=11/13$) (Fig. 8C,D). Interestingly, in none of the TAB-supplemented cultures (either from the BMS493 or the *Raldh2*^{-/-} model) did the rescue of lung buds occur bilaterally. Whether the right or the left lung was rescued was not determined. Presumably, it was the right lung, because other RA-deficient models (*Rara/Rarb*-null mice, vitamin A-deficient rats, and *Raldh2*^{-/-} embryos rescued with low RA doses) characteristically show left lung agenesis and right lung hypoplasia (Mendelsohn et al., 1994; Wang et al., 2006; Wilson et al., 1953).

How could TAB prevent the total lung agenesis characteristic of the RA-deficient foreguts? WMISH assessment of *Fgf10* expression confirmed that this gene is selectively downregulated in the lung field of foregut cultures treated with BMS493 alone, as previously reported (Desai et al., 2004). The local disruption of *Fgf10* by BMS493 contrasted with the strong *Fgf10* expression associated with the rescued lung bud in BMS493 plus TAB-treated foreguts (Fig. 8E,F). Nevertheless, the distribution of *Fgf10* mRNA in the lung field in these cultures was overall more diffuse than in control foreguts (compare with Fig. 5C). This is likely to have contributed to the prevention of full rescue of the lung phenotype in BMS493 plus TAB-treated cultures. Endogenous RA may be crucial in establishing local gradients of signaling molecules, such as Fgf10, in the prospective lung field. Our data support a model in which endogenous RA maintains low levels of Tgf β signaling in the lung field to allow proper expression of *Fgf10* and initiation of lung bud morphogenesis (Fig. 9).

DISCUSSION

In the present study, we provide evidence of a novel mechanism implicating RA-Tgf β -Fgf10 interactions in initiation of lung morphogenesis. Regulation of Tgf β signaling by RA has been extensively reported, but data are overall conflicting. In some cell lines, RA increases production of Tgf β 1 and its receptors, leading to growth inhibition (Batova et al., 1992; Danielpour, 1996; Falk et al., 1991; Glick et al., 1989; Imai et al., 1997; Kojima and Rifkin, 1993). RA, however, has also been reported to inhibit endogenous Tgf β signaling in the mesenchyme of the developing inner ear (Frenz and Liu, 2000) and palate (Yu and Xing, 2006) in mice. Disruption of *Rxra* in mice results in abnormal upregulation of *Tgfb2* in cardiac tissue (Kubalak et al., 2002). A microarray analysis of vitamin A-deficient rat embryos revealed upregulation of some of the genes (such as procollagens) found in our study, suggestive of increased Tgf β -dependent activity (Flentke et al., 2004). By contrast, in the yolk sac, disruption of RA signaling inhibits Tgf β -dependent expression of fibronectin and integrin and disrupts visceral endoderm and vascular development (Bohnsack et al.,

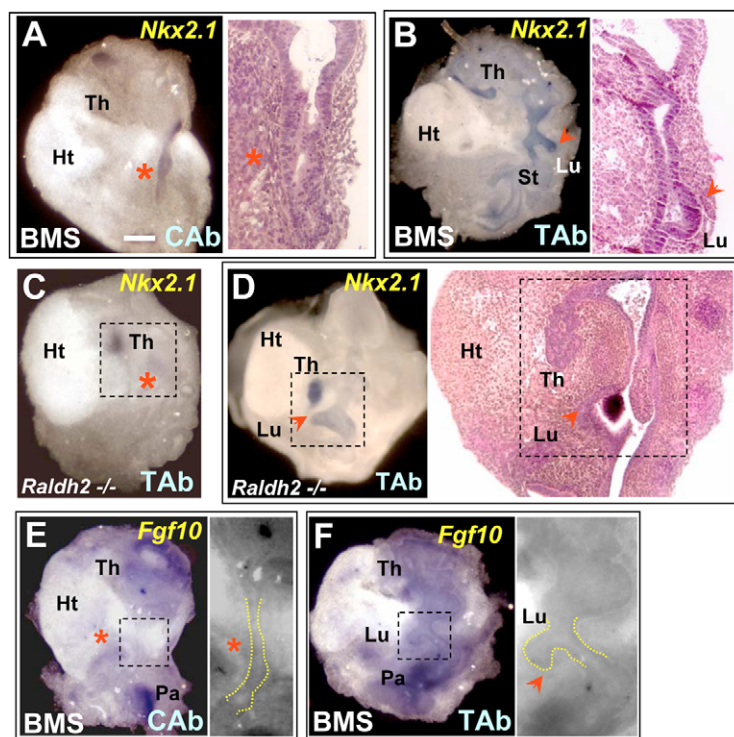


Fig. 8. Blocking Tgfb signaling rescues bud formation and gene expression in the lung field of RA-deficient foregut. (A-D) BMS493-treated mouse foregut fails to induce lung bud formation (A, asterisks; E, asterisk, boxed region). However, treatment with a combination of BMS493 and pan-specific TGF β -blocking antibody (TAb) allows bud formation and strong *Nkx2.1* signals are detected in the prospective lung region of the WT foregut (B, arrowheads). (C,D) Similarly, untreated *Raldh2*^{-/-} foregut does not form lung buds under the control condition (C, asterisk), but budding and *Nkx2.1* expression are partially rescued by TAb treatment (D, arrowheads). (E,F) In BMS493-treated WT foregut, *Fgf10* mRNA is seen in the thyroid and pancreatic fields, but not in the prospective lung region (E, boxed area). In WT foregut treated with both BMS493 and TAb, there is strong *Fgf10* expression (F, boxed area) associated with the rescued lung bud (F, arrowhead). Panels to the right are the corresponding enhanced-contrast images of the explants in E and F. Th, thyroid; Ht, heart; Lu, lung; Pa, pancreas; CAb, unrelated isotype-matched control antibody. Scale bar: 270 μ m in A.

2004). The discordant data suggest that the way RA and Tgfb interact is strongly influenced by the local milieu and thus depends on the particular system studied.

Our finding of negative regulation of the Tgfb pathway by RA was supported by results from multiple approaches in two highly relevant models. These included identification of a number of Tgfb targets differentially expressed in RA-deficient foreguts by microarray analysis, with further confirmation of their expression pattern, and changes in Smad2 phosphorylation. It was noteworthy that a number of Tgfb targets involved in synthesis, binding or remodeling of extracellular matrix components, such as Ctgf, Cyr61, Col1a, Col3a1, Pcolce, Timp1 and Timp3, were upregulated in RA-deficient foreguts. We could only speculate, but not prove, that increased matrix deposition and presumably fibrosis could have a negative effect in epithelial-mesenchymal interactions and bud induction. Our study, however, strongly suggests that the underlying reason for disruption of lung formation due to hyperactive Tgfb signaling is the Tgfb-mediated downregulation of *Fgf10*.

Although under RA-deficient conditions our microarray analysis showed upregulation of the Tgfb signaling transducing elements *Tgfb1* and *Smad4* ($P < 0.05$ in both), we could not determine precisely how the Tgfb pathway was influenced by endogenous RA. Presumably, an increase in the amount of Tgfb1 could increase the number of functional receptor complexes to enhance signaling. Nevertheless, an equivalent increase in expression of Tgfb2, the receptor that binds to and phosphorylates Tgfb1 (Bartram and Speer, 2004), was not observed. Moreover, at the mRNA level, none of the Tgfb ligands was upregulated by loss of RA signaling (data not shown). We considered the possibility that a RA-regulated mechanism leading to conversion of latent Tgfb ligand into an active form could be enhanced in RA-deficient foreguts. This idea was attractive, as several genes associated with this function were differentially upregulated by RA deficiency in both models, such as annexin A2, cathepsin H, mannose-6-phosphate receptor, matrix

metallopeptidase 9 and S100 calcium binding protein A10 (Harpel et al., 1993; Krishnan et al., 2004; Ling et al., 2004; Lyons et al., 1988; Nunes et al., 1997; Rifkin et al., 1997; Taipale et al., 1994; Yu and Stamenkovic, 2000; Zhang et al., 2004) (F.C. and W.V.C., unpublished). Using an immunofluorescence protocol to detect latent and active TGF β 1 (Ewan et al., 2002), we could not identify significant differences in staining pattern that could account for the major changes described here. Demonstration of active Tgfb ligand is technically challenging, even when Tgfb signaling is evident, in part owing to the short half-life of the active Tgfb ligand (Araya et al., 2006; Flanders et al., 2001; Wakefield et al., 1990). In our RA-

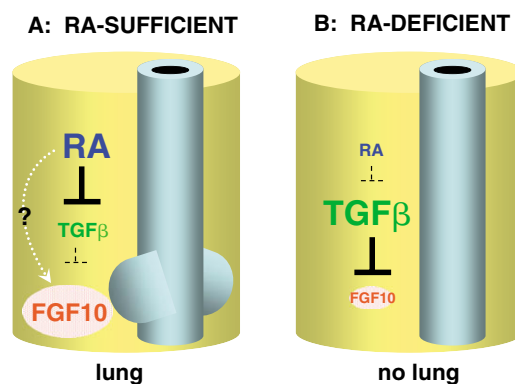


Fig. 9. RA-Tgfb-Fgf10 interactions during primary lung bud formation in the mouse. (A) In an RA-sufficient foregut, endogenous RA maintains low levels of Tgfb signaling in the mesoderm of the lung field to allow *Fgf10* expression and lung bud initiation. (B) Under conditions of RA-deficiency, Tgfb signaling is abnormally hyperactivated, thereby blocking *Fgf10* expression and lung bud formation.

deficient foreguts, it is possible that the activation of Tgf β signaling would require only minimal increase in the active Tgf β ligand, as at least one of the Tgf β receptors is also being upregulated. Further studies will be required to clarify these issues.

We thank Pascal Dollé, Janet Rossant, Robert Kelly and Saverio Bellusci for providing us with the *Raldh2*^{-/-}, *RARElacZ* and *Fgf10lacZ* mice, respectively; Chris Zusi (Bristol Myers Squibb) for the pan-RAR antagonist BMS493; Parviz Minoo, Andrew McMahon, Nobuyuki Itoh and Harold Moses for cDNA clones; and Chun Li and Xiuzhi Tang for their excellent technical assistance. This work was supported by grants from NIH/NHLBI (F32 HL080846, R01 HL67129 and P01 HL47049) and the GlaxoSmithKline Pulmonary Fellowship Award.

References

- Araya, J., Cambier, S., Morris, A., Finkbeiner, W. and Nishimura, S. L. (2006). Integrin-mediated transforming growth factor-beta activation regulates homeostasis of the pulmonary epithelial-mesenchymal trophic unit. *Am. J. Pathol.* **169**, 405-415.
- Bartholin, L., Wessner, L. L., Chirgwin, J. M. and Guise, T. A. (2007). The human Cyr61 gene is a transcriptional target of transforming growth factor beta in cancer cells. *Cancer Lett.* **246**, 230-236.
- Bartram, U. and Speer, C. P. (2004). The role of transforming growth factor beta in lung development and disease. *Chest* **125**, 754-765.
- Batova, A., Danielpour, D., Pirisi, L. and Creek, K. E. (1992). Retinoic acid induces secretion of latent transforming growth factor beta 1 and beta 2 in normal and human papillomavirus type 16-immortalized human keratinocytes. *Cell Growth Differ.* **3**, 763-772.
- Beer, H. D., Florence, C., Dammeier, J., McGuire, L., Werner, S. and Duan, D. R. (1997). Mouse fibroblast growth factor 10, cDNA cloning, protein characterization, and regulation of mRNA expression. *Oncogene* **15**, 2211-2218.
- Benson, M., Carlsson, B., Carlsson, L. M., Mostad, P., Svensson, P. A. and Cardell, L. O. (2002). DNA microarray analysis of transforming growth factor-beta and related transcripts in nasal biopsies from patients with allergic rhinitis. *Cytokine* **18**, 20-25.
- Bertelli, R., Valenti, F., Oleggini, R., Caridi, G., Altieri, P., Coviello, D. A., Botti, G., Ravazzolo, R. and Ghiggeri, G. M. (1998). Cell-specific regulation of alpha1(III) and alpha2(V) collagen by TGF-beta1 in tubulointerstitial cell models. *Nephrol. Dial. Transplant.* **13**, 573-579.
- Billings, P. C., Whitbeck, J. C., Adams, C. S., Abrams, W. R., Cohen, A. J., Engelsberg, B. N., Howard, P. S. and Rosenbloom, J. (2002). The transforming growth factor-beta-inducible matrix protein (beta)ig-h3 interacts with fibronectin. *J. Biol. Chem.* **277**, 28003-28009.
- Bohnsack, B. L., Lai, L., Dolle, P. and Hirschi, K. K. (2004). Signaling hierarchy downstream of retinoic acid that independently regulates vascular remodeling and endothelial cell proliferation. *Genes Dev.* **18**, 1345-1358.
- Cardoso, W. V. and Lu, J. (2006). Regulation of early lung morphogenesis: questions, facts and controversies. *Development* **133**, 1611-1624.
- Chambon, P. (1996). A decade of molecular biology of retinoic acid receptors. *FASEB J.* **10**, 940-954.
- Chen, W. B., Lenschow, W., Tiede, K., Fischer, J. W., Kalthoff, H. and Ungefroren, H. (2002). Smad4/DPC4-dependent regulation of biglycan gene expression by transforming growth factor-beta in pancreatic tumor cells. *J. Biol. Chem.* **277**, 36118-36128.
- Chuva de Sousa Lopes, S. M., Feijen, A., Korving, J., Korchynskiy, O., Larsson, J., Karlsson, S., ten Dijke, P., Lyons, K. M., Goldschmeding, R., Doevendans, P. et al. (2004). Connective tissue growth factor expression and Smad signaling during mouse heart development and myocardial infarction. *Dev. Dyn.* **231**, 542-550.
- Clagett-Dame, M. and DeLuca, H. F. (2002). The role of vitamin A in mammalian reproduction and embryonic development. *Annu. Rev. Nutr.* **22**, 347-381.
- Colwell, A. S., Krummel, T. M., Longaker, M. T. and Lorenz, H. P. (2006). Fetal and adult fibroblasts have similar TGF-beta-mediated, Smad-dependent signaling pathways. *Plast. Reconstr. Surg.* **117**, 2277-2283.
- Dahlfors, G. and Arnqvist, H. J. (2000). Vascular endothelial growth factor and transforming growth factor-beta1 regulate the expression of insulin-like growth factor-binding protein-3, -4, and -5 in large vessel endothelial cells. *Endocrinology* **141**, 2062-2067.
- Danielpour, D. (1996). Induction of transforming growth factor-beta autocrine activity by all-trans-retinoic acid and 1 alpha,25-dihydroxyvitamin D3 in NRP-152 rat prostatic epithelial cells. *J. Cell. Physiol.* **166**, 231-239.
- de Jong, D. S., van Zoelen, E. J., Bauerschmidt, S., Olijve, W. and Steegenga, W. T. (2002). Microarray analysis of bone morphogenetic protein, transforming growth factor beta, and activin early response genes during osteoblastic cell differentiation. *J. Bone Miner. Res.* **17**, 2119-2129.
- de Sousa Lopes, S. M., Carvalho, R. L., van den Driesche, S., Goumans, M. J., ten Dijke, P. and Mummery, C. L. (2003). Distribution of phosphorylated Smad2 identifies target tissues of TGF beta ligands in mouse development. *Gene Expr. Patterns* **3**, 355-360.
- Desai, T. J., Malpel, S., Flentke, G. R., Smith, S. M. and Cardoso, W. V. (2004). Retinoic acid selectively regulates Fgf10 expression and maintains cell identity in the prospective lung field of the developing foregut. *Dev. Biol.* **273**, 402-415.
- Desai, T. J., Chen, F., Lu, J., Qian, J., Niederreither, K., Dolle, P., Chambon, P. and Cardoso, W. V. (2006). Distinct roles for retinoic acid receptors alpha and beta in early lung morphogenesis. *Dev. Biol.* **291**, 12-24.
- Dickman, E. D., Thaller, C. and Smith, S. M. (1997). Temporally-regulated retinoic acid depletion produces specific neural crest, ocular and nervous system defects. *Development* **124**, 3111-3121.
- Ewan, K. B., Shyamala, G., Ravani, S. A., Tang, Y., Akhurst, R., Wakefield, L. and Barcellos-Hoff, M. H. (2002). Latent transforming growth factor-beta activation in mammary gland: regulation by ovarian hormones affects ductal and alveolar proliferation. *Am. J. Pathol.* **160**, 2081-2093.
- Falk, L. A., De Benedetti, F., Lohrey, N., Birchenall-Roberts, M. C., Ellingsworth, L. W., Faltynek, C. R. and Ruscetti, F. W. (1991). Induction of transforming growth factor-beta 1 (TGF-beta 1), receptor expression and TGF-beta 1 protein production in retinoic acid-treated HL-60 cells: possible TGF-beta 1-mediated autocrine inhibition. *Blood* **77**, 1248-1255.
- Ferguson, J. W., Mikesch, M. F., Wheeler, E. F. and LeBaron, R. G. (2003). Developmental expression patterns of Beta-ig (betaIG-H3) and its function as a cell adhesion protein. *Mech. Dev.* **120**, 851-864.
- Flanders, K. C., Kim, E. S. and Roberts, A. B. (2001). Immunohistochemical expression of Smads 1-6 in the 15-day gestation mouse embryo: signaling by BMPs and TGF-betas. *Dev. Dyn.* **220**, 141-154.
- Flentke, G. R., Baker, M. W., Docterman, K. E., Power, S., Lough, J. and Smith, S. M. (2004). Microarray analysis of retinoid-dependent gene activity during rat embryogenesis: increased collagen fibril production in a model of retinoid insufficiency. *Dev. Dyn.* **229**, 886-898.
- Frenz, D. A. and Liu, W. (2000). Treatment with all-trans-retinoic acid decreases levels of endogenous TGF-beta(1) in the mesenchyme of the developing mouse inner ear. *Teratology* **61**, 297-304.
- Fujita, T., Shiba, H., Sakata, M., Uchida, Y., Ogawa, T. and Kurihara, H. (2002). Effects of transforming growth factor-beta 1 and fibronectin on SPARC expression in cultures of human periodontal ligament cells. *Cell Biol. Int.* **26**, 1065-1072.
- Glick, A. B., Flanders, K. C., Danielpour, D., Yuspa, S. H. and Sporn, M. B. (1989). Retinoic acid induces transforming growth factor-beta 2 in cultured keratinocytes and mouse epidermis. *Cell Regul.* **1**, 87-97.
- Groth, S., Schulze, M., Kalthoff, H., Fandrich, F. and Ungefroren, H. (2005). Adhesion and Rac1-dependent regulation of biglycan gene expression by transforming growth factor-beta. Evidence for oxidative signaling through NADPH oxidase. *J. Biol. Chem.* **280**, 33190-33199.
- Harpel, M. R., Lee, E. H. and Hartman, F. C. (1993). Anion-exchange analysis of ribulose-bisphosphate carboxylase/oxygenase reactions: CO2/O2 specificity determination and identification of side products. *Anal. Biochem.* **209**, 367-374.
- Imai, S., Okuno, M., Moriwaki, H., Muto, Y., Murakami, K., Shudo, K., Suzuki, Y. and Kojima, S. (1997). 9,13-di-cis-Retinoic acid induces the production of tPA and activation of latent TGF-beta via RAR alpha in a human liver stellate cell line, L190. *FEBS Lett.* **411**, 102-106.
- Kang, Y., Chen, C. R. and Massague, J. (2003). A self-enabling TGFbeta response coupled to stress signaling: Smad engages stress response factor ATF3 for Id1 repression in epithelial cells. *Mol. Cell* **11**, 915-926.
- Kapoun, A. M., Liang, F., O'Young, G., Damm, D. L., Quon, D., White, R. T., Munson, K., Lam, A., Schreiner, G. F. and Protter, A. A. (2004). B-type natriuretic peptide exerts broad functional opposition to transforming growth factor-beta in primary human cardiac fibroblasts: fibrosis, myofibroblast conversion, proliferation, and inflammation. *Circ. Res.* **94**, 453-461.
- Kastner, P., Mark, M., Ghyselinck, N., Krezel, W., Dupe, V., Gronoda, J. M. and Chambon, P. (1997). Genetic evidence that the retinoid signal is transduced by heterodimeric RXR/RAR functional units during mouse development. *Development* **124**, 313-326.
- Kelly, R. G., Brown, N. A. and Buckingham, M. E. (2001). The arterial pole of the mouse heart forms from Fgf10-expressing cells in pharyngeal mesoderm. *Dev. Cell* **1**, 435-440.
- Kojima, S. and Rifkin, D. B. (1993). Mechanism of retinoid-induced activation of latent transforming growth factor-beta in bovine endothelial cells. *J. Cell. Physiol.* **155**, 323-332.
- Krishnan, S., Deora, A. B., Annes, J. P., Osoria, J., Rifkin, D. B. and Hajjar, K. A. (2004). Annexin II-mediated plasmin generation activates TGF-beta3 during epithelial-mesenchymal transformation in the developing avian heart. *Dev. Biol.* **265**, 140-154.
- Kubalak, S. W., Hutson, D. R., Scott, K. K. and Shannon, R. A. (2002). Elevated transforming growth factor beta2 enhances apoptosis and contributes to abnormal outflow tract and aortic sac development in retinoic X receptor alpha knockout embryos. *Development* **129**, 733-746.
- Leask, A. and Abraham, D. J. (2003). The role of connective tissue growth factor, a multifunctional matricellular protein, in fibroblast biology. *Biochem. Cell Biol.* **81**, 355-363.
- LeBaron, R. G., Bezverkov, K. I., Zimmer, M. P., Pavelec, R., Skonier, J. and Purchio, A. F. (1995). Beta IG-H3, a novel secretory protein inducible by transforming growth factor-beta, is present in normal skin and promotes the

- adhesion and spreading of dermal fibroblasts in vitro. *J. Invest. Dermatol.* **104**, 844-849.
- Lebeche, D., Malpel, S. and Cardoso, W. V.** (1999). Fibroblast growth factor interactions in the developing lung. *Mech. Dev.* **86**, 125-136.
- Leivonen, S. K., Hakkinen, L., Liu, D. and Kahari, V. M.** (2005). Smad3 and extracellular signal-regulated kinase 1/2 coordinately mediate transforming growth factor-beta-induced expression of connective tissue growth factor in human fibroblasts. *J. Invest. Dermatol.* **124**, 1162-1169.
- Letterio, J. J., Geiser, A. G., Kulkarni, A. B., Roche, N. S., Sporn, M. B. and Roberts, A. B.** (1994). Maternal rescue of transforming growth factor-beta 1 null mice. *Science* **264**, 1936-1938.
- Ling, Q., Jacovina, A. T., Deora, A., Febbraio, M., Simantov, R., Silverstein, R. L., Hempstead, B., Mark, W. H. and Hajjar, K. A.** (2004). Annexin II regulates fibrin homeostasis and neoangiogenesis in vivo. *J. Clin. Invest.* **113**, 38-48.
- Lu, J., Qian, J., Izvolsky, K. I. and Cardoso, W. V.** (2004). Global analysis of genes differentially expressed in branching and non-branching regions of the mouse embryonic lung. *Dev. Biol.* **273**, 418-435.
- Lyons, R. M., Keski-Oja, J. and Moses, H. L.** (1988). Proteolytic activation of latent transforming growth factor-beta from fibroblast-conditioned medium. *J. Cell Biol.* **106**, 1659-1665.
- Mailleux, A. A., Kelly, R., Veltmaat, J. M., De Langhe, S. P., Zaffran, S., Thiery, J. P. and Bellusci, S.** (2005). Fgf10 expression identifies parabronchial smooth muscle cell progenitors and is required for their entry into the smooth muscle cell lineage. *Development* **132**, 2157-2166.
- Malpel, S., Mendelsohn, C. and Cardoso, W. V.** (2000). Regulation of retinoic acid signaling during lung morphogenesis. *Development* **127**, 3057-3067.
- Mendelsohn, C., Lohnes, D., Decimo, D., Lufkin, T., LeMeur, M., Chambon, P. and Mark, M.** (1994). Function of the retinoic acid receptors (RARs) during development (II). Multiple abnormalities at various stages of organogenesis in RAR double mutants. *Development* **120**, 2749-2771.
- Millan, F. A., Denhez, F., Kondaiah, P. and Akhurst, R. J.** (1991). Embryonic gene expression patterns of TGF beta 1, beta 2 and beta 3 suggest different developmental functions in vivo. *Development* **111**, 131-143.
- Min, H., Danilenko, D. M., Scully, S. A., Bolon, B., Ring, B. D., Tarpley, J. E., DeRose, M. and Simonet, W. S.** (1998). Fgf-10 is required for both limb and lung development and exhibits striking functional similarity to Drosophila branchless. *Genes Dev.* **12**, 3156-3161.
- Minoo, P., Su, G., Drum, H., Bringas, P. and Kimura, S.** (1999). Defects in tracheoesophageal and lung morphogenesis in Nkx2.1(-/-) mouse embryos. *Dev. Biol.* **209**, 60-71.
- Mollard, R., Ghyselinck, N. B., Wendling, O., Chambon, P. and Mark, M.** (2000a). Stage-dependent responses of the developing lung to retinoic acid signaling. *Int. J. Dev. Biol.* **44**, 457-462.
- Mollard, R., Viville, S., Ward, S. J., Decimo, D., Chambon, P. and Dolle, P.** (2000b). Tissue-specific expression of retinoic acid receptor isoform transcripts in the mouse embryo. *Mech. Dev.* **94**, 223-232.
- Niederreither, K., Subbarayan, V., Dolle, P. and Chambon, P.** (1999). Embryonic retinoic acid synthesis is essential for early mouse post-implantation development. *Nat. Genet.* **21**, 444-448.
- Nunes, I., Gleizes, P. E., Metz, C. N. and Rifkin, D. B.** (1997). Latent transforming growth factor-beta binding protein domains involved in activation and transglutaminase-dependent cross-linking of latent transforming growth factor-beta. *J. Cell Biol.* **136**, 1151-1163.
- Okano, K., Schnaper, H. W., Bomsztyk, K. and Hayashida, T.** (2006). RACK1 binds to Smad3 to modulate TGF-beta 1-stimulated alpha 2(I) collagen transcription in renal tubular epithelial cells. *J. Biol. Chem.* **281**, 26196-26204.
- Olsen, D., Yang, C., Bodo, M., Chang, R., Leigh, S., Baez, J., Carmichael, D., Perala, M., Hamalainen, E. R., Jarvinen, M. et al.** (2003). Recombinant collagen and gelatin for drug delivery. *Adv. Drug Deliv. Rev.* **55**, 1547-1567.
- Pavasant, P., Yongchaitrakul, T., Pattamapun, K. and Arksornnukit, M.** (2003). The synergistic effect of TGF-beta and 1,25-dihydroxyvitamin D3 on SPARC synthesis and alkaline phosphatase activity in human pulp fibroblasts. *Arch. Oral Biol.* **48**, 717-722.
- Ponticos, M., Abraham, D., Alexakis, C., Lu, Q. L., Black, C., Partridge, T. and Bou-Gharios, G.** (2004). Col1a2 enhancer regulates collagen activity during development and in adult tissue repair. *Matrix Biol.* **22**, 619-628.
- Rifkin, D. B., Gleizes, P. E., Harpel, J., Nunes, I., Munger, J., Mazzieri, R. and Noguera, I.** (1997). Plasminogen/plasminogen activator and growth factor activation. *Ciba Found. Symp.* **212**, 105-115.
- Roelen, B. A., Lin, H. Y., Knezevic, V., Freund, E. and Mummery, C. L.** (1994). Expression of TGF-beta s and their receptors during implantation and organogenesis of the mouse embryo. *Dev. Biol.* **166**, 716-728.
- Rossant, J., Zirngibl, R., Cado, D., Shago, M. and Giguere, V.** (1991). Expression of a retinoic acid response element-hsplacZ transgene defines specific domains of transcriptional activity during mouse embryogenesis. *Genes Dev.* **5**, 1333-1344.
- Schmid, P., Cox, D., Bilbe, G., Maier, R. and McMaster, G. K.** (1991). Differential expression of TGF beta 1, beta 2 and beta 3 genes during mouse embryogenesis. *Development* **111**, 117-130.
- Schneider, D., Kleeff, J., Berberat, P. O., Zhu, Z., Korc, M., Friess, H. and Buchler, M. W.** (2002). Induction and expression of betaig-h3 in pancreatic cancer cells. *Biochim. Biophys. Acta* **1588**, 1-6.
- Sekine, K., Ohuchi, H., Fujiwara, M., Yamasaki, M., Yoshizawa, T., Sato, T., Yagishita, N., Matsui, D., Koga, Y., Itoh, N. et al.** (1999). Fgf10 is essential for limb and lung formation. *Nat. Genet.* **21**, 138-141.
- Shalitin, N., Schlesinger, H., Levy, M. J., Kessler, E. and Kessler-Ickson, G.** (2003). Expression of procollagen C-proteinase enhancer in cultured rat heart fibroblasts: evidence for co-regulation with type I collagen. *J. Cell Biochem.* **90**, 397-407.
- Shannon, J. M. and Hyatt, B. A.** (2004). Epithelial-mesenchymal interactions in the developing lung. *Annu. Rev. Physiol.* **66**, 625-645.
- Skonier, J., Bennett, K., Rothwell, V., Kosowski, S., Plowman, G., Wallace, P., Edelhoff, S., Disteche, C., Neubauer, M., Marquardt, H. et al.** (1994). beta ig-h3: a transforming growth factor-beta-responsive gene encoding a secreted protein that inhibits cell attachment in vitro and suppresses the growth of CHO cells in nude mice. *DNA Cell Biol.* **13**, 571-584.
- Sodek, J., Chen, J., Nagata, T., Kasugai, S., Todescan, R., Jr, Li, I. W. and Kim, R. H.** (1995). Regulation of osteopontin expression in osteoblasts. *Ann. N. Y. Acad. Sci.* **760**, 223-241.
- Taipale, J., Miyazono, K., Heldin, C. H. and Keski-Oja, J.** (1994). Latent transforming growth factor-beta 1 associates to fibroblast extracellular matrix via latent TGF-beta binding protein. *J. Cell Biol.* **124**, 171-181.
- Tomlinson, D. C., Grindley, J. C. and Thomson, A. A.** (2004). Regulation of Fgf10 gene expression in the prostate: identification of transforming growth factor-beta1 and promoter elements. *Endocrinology* **145**, 1988-1995.
- Ungefroren, H., Lenschow, W., Chen, W. B., Faendrich, F. and Kalthoff, H.** (2003). Regulation of biglycan gene expression by transforming growth factor-beta requires MKK6-p38 mitogen-activated protein Kinase signaling downstream of Smad signaling. *J. Biol. Chem.* **278**, 11041-11049.
- Verrecchia, F., Chu, M. L. and Mauviel, A.** (2001). Identification of novel TGF-beta/Smad gene targets in dermal fibroblasts using a combined cDNA microarray/promoter transactivation approach. *J. Biol. Chem.* **276**, 17058-17062.
- Wakefield, L. M., Winokur, T. S., Hollands, R. S., Christopherson, K., Levinson, A. D. and Sporn, M. B.** (1990). Recombinant latent transforming growth factor beta 1 has a longer plasma half-life in rats than active transforming growth factor beta 1, and a different tissue distribution. *J. Clin. Invest.* **86**, 1976-1984.
- Wang, Z., Dolle, P., Cardoso, W. V. and Niederreither, K.** (2006). Retinoic acid regulates morphogenesis and patterning of posterior foregut derivatives. *Dev. Biol.* **297**, 433-445.
- Wells, J. M. and Melton, D. A.** (1999). Vertebrate endoderm development. *Annu. Rev. Cell Dev. Biol.* **15**, 393-410.
- Wendling, O., Dennefeld, C., Chambon, P. and Mark, M.** (2000). Retinoid signaling is essential for patterning the endoderm of the third and fourth pharyngeal arches. *Development* **127**, 1553-1562.
- Wertz, K. and Herrmann, B. G.** (2000). Large-scale screen for genes involved in gonad development. *Mech. Dev.* **98**, 51-70.
- Wilson, J. G., Roth, C. B. and Warkany, J.** (1953). An analysis of the syndrome of malformations induced by maternal vitamin A deficiency. Effects of restoration of vitamin A at various times during gestation. *Am. J. Anat.* **92**, 189-217.
- Xie, L., Law, B. K., Aakre, M. E., Edgerton, M., Shyr, Y., Bhowmick, N. A. and Moses, H. L.** (2003). Transforming growth factor beta-regulated gene expression in a mouse mammary gland epithelial cell line. *Breast Cancer Res.* **5**, R187-R198.
- Yu, Q. and Stamenkovic, I.** (2000). Cell surface-localized matrix metalloproteinase-9 proteolytically activates TGF-beta and promotes tumor invasion and angiogenesis. *Genes Dev.* **14**, 163-176.
- Yu, Z. and Xing, Y.** (2006). All-trans retinoic acid inhibited chondrogenesis of mouse embryonic palate mesenchymal cells by down-regulation of TGF-beta/Smad signaling. *Biochem. Biophys. Res. Commun.* **340**, 929-934.
- Yun, S. J., Kim, M. O., Kim, S. O., Park, J., Kwon, Y. K., Kim, I. S. and Lee, E. H.** (2002). Induction of TGF-beta-inducible gene-h3 (betaig-h3) by TGF-beta1 in astrocytes: implications for astrocyte response to brain injury. *Brain Res. Mol. Brain Res.* **107**, 57-64.
- Zhang, L., Fogg, D. K. and Waisman, D. M.** (2004). RNA interference-mediated silencing of the S100A10 gene attenuates plasmin generation and invasiveness of Colo 222 colorectal cancer cells. *J. Biol. Chem.* **279**, 2053-2062.